Characteristics and Performance of a Mesoporous Cerium-Aluminum-Silver Mixed Oxide for Removal of Methyl Violet Dye
(Pencirian dan Prestasi Campuran Oksida Mesoberliang Serium-Aluminum-Perak untuk Menanggalkan Pewarna Metil Ungu)

PHATAI, P.* & SRISOMANG, R.

ABSTRACT

In this study, the adsorption efficiency of methyl violet (MV) dye onto $Ce_{0.3}Al_{0.7}$ and $Ce_{0.3}Al_{0.7}Ag_x$ (x = 0.1, 0.3 & 0.5) mixed oxides was investigated. The properties of mixed oxide were determined by X-ray diffraction (XRD), Fourier transform infrared spectroscopy (FTIR), scanning electron microscopy (SEM), energy dispersive X-ray spectroscopy (EDX), N_2 adsorption-desorption isotherm, diffuse reflectance UV-vis spectroscopy (UV-vis DRS) and X-ray absorption near edge structure (XANES). Characterization showed that synthesized mixed oxide with fluorite has a pure cubic structure of a mesoporous nature and a small grain size with rough surface. Batch adsorption experiments were used to study parameters including contact time and initial dye concentration. The results showed that these parameters affected the degree of MV dye adsorption. The dye adsorption of mixed oxides attained equilibrium at 120 min. The equilibrium adsorption data were analyzed using Langmuir, Freundlich and Temkin isotherms. The adsorption behavior of MV dye onto $Ce_{0.3}Al_{0.7}$ was found to follow the Langmuir isotherm (R^2 = 0.9951), providing a maximum monolayer adsorptive capacity of 2.35 mg/g. Alternatively, the adsorption of MV dye onto $Ce_{0.3}Al_{0.7}Ag_{0.1}$ (R^2 = 0.7839), $Ce_{0.3}Al_{0.7}Ag_{0.3}$ (R^2 = 0.9301) and $Ce_{0.3}Al_{0.7}Ag_{0.5}$ (R^2 = 0.9396) followed the Freundlich isotherm. The possible adsorption mechanisms of MV dyes onto the $Ce_{0.3}Al_{0.7}$ and $Ce_{0.3}Al_{0.7}Ag_x$ were also discussed.

Keywords: Cerium & aluminum mixed oxides; Langmuir isotherm; methyl violet dye; silver

ABSTRAK

Dalam penyelidikan ini, kecekapan penjerapan pewarna metil ungu (MV) ke atas $Ce_{0.3}Al_{0.7}$ dan $Ce_{0.3}Al_{0.7}Ag_x$ (x = 0.1, 0.3 & 0.5) campuran oksida dikaji. Sifat campuran oksida telah ditetapkan melalui pembelauan sinar-x (XRD), spektroskopi transformasi Fourier inframerah (FTIR), mikroskop elektron imbasan (SEM), spektroskopi serakan tenaga sinar-x (EDX), N_2 penjerapan-penyahjerapan isoterma, meresap pemantulan UV-vis spektroskopi (DRS UV-vis) serta penyerapan X-ray berhampiran sisi struktur (XANES). Pencirian menunjukkan bahawa sintesis campuran oksida dengan fluorit mempunyai struktur padu tulen bersifat mesoporous dan saiz kecil bijirin dengan permukaan yang kasar. Kelompok penjerapan eksperimen telah digunakan untuk mengkaji parameter termasuk hubungan masa dan tumpuan awal pewarna. Hasil kajian menunjukkan bahawa parameter ini menjejaskan tahap penjerapan pewarna MV. Penjerapan pewarna daripada campuran oksida mencapai keseimbangan pada 120 min. Keseimbangan penjerapan data dianalisis menggunakan isoterma Langmuir, Freundlich dan Temkin. Perlakuan penjerapan pewarna MV ke dalam $Ce_{0.3}Al_{0.7}$ dilihat mengikuti isoterma Langmuir (R^2 = 0.9951), menyediakan kapasiti penjerapan maksimum monolapisan 2.35 mg/g. Sebagai alternatif, penjerapan daripada pewarna MV ke dalam $Ce_{0.3}Al_{0.7}Ag_{0.1}$ (R^2 = 0.7839), $Ce_{0.3}Al_{0.7}Ag_{0.3}$ (R^2 = 0.9301) dan $Ce_{0.3}Al_{0.7}Ag_{0.5}$ (R^2 = 0.9396) diikuti isoterma Freundlich. Mekanisme penjerapan munasabah pewarna MV ke dalam $Ce_{0.3}Al_{0.7}$ dan $Ce_{0.3}Al_{0.7}Ag_x$ juga turut dibincangkan.

Kata kunci: Campuran oksida serium & aluminium; isoterma Langmuir; perak; pewarna metil ungu

INTRODUCTION

Dyes and pigments are usually applied in the paper, plastics, leather, food and textile industries. The discharge of colored wastewater from these industries may cause an ecotoxic hazard. Dye contamination of water affects photosynthetic processes of aquatic plants, which reduces oxygen levels in water. Methyl violet (MV) is a particularly important dye because of its wide applications in textiles, paints and inks (Monash & Pugazhenthi 2009). The presence of MV dye in surface water and groundwater can cause significant public health problems such as irritated eyes, skin and respiratory tracts. Consequently, it must be removed before it was discharged into receiving streams (Mittal et al. 2008).

The removal of dyes from aqueous environments has been extensively investigated. Various methods such as advanced oxidation processes (AOPs) (Guimarães et al. 2012), catalysis (Tapalad et al. 2008) and adsorption (Kongkachuichay et al. 2010) have been used. Among these methods, adsorption technology has been

extensively employed because this method is simple, economical, flexible, easy to use and inexpensive (Deniz 2013). Several porous adsorbents have been investigated for their effectiveness in adsorptive removal of dyes from aqueous solutions by comparing them to traditional adsorbents such as activated carbon (Phatai et al. 2014; Zaini et al. 2014), agricultural wastes (Subramaniam & Ponnusamy 2015) and mixed oxides (Debnath et al. 2014; Jiao et al. 2014; Phatai & Futalan 2016; Wawrzkiewicz et al. 2015). The application of some of these adsorbents was restricted due to their high costs, problematic disposal processes and regeneration. Mixed metal oxides are oxide groups consisting of two or more cation species. The efficiency of mixed oxides such as SiO_2-Al_2O_3 (Wawrzkiewicz et al. 2015), Mg-Al (Jiao et al. 2014) and Ca-Fe (Debnath et al. 2014), in removal of dye molecules has been reported in recent years. In our previous research (Phatai & Futalan 2016), Ce_xAl_{1-x} (x = 0.3, 0.5 & 0.7) mixed oxides have been applied in the adsorption of MV dye. Our results showed that $Ce_{0.3}Al_{0.7}$ gave the best adsorption efficiency at pH9.0. In order to increase the MV adsorption capacity of $Ce_{0.3}Al_{0.7}$, silver ions (Ag^+) were incorporated into the lattice structure of $Ce_{0.3}Al_{0.7}$ oxide.

This study aimed to investigate the removal of MV by adsorption onto $Ce_{0.3}Al_{0.7}$ and $Ce_{0.3}Al_{0.7}Ag_x$ (x = 0.1, 0.3 & 0.5) oxides under different experimental conditions, varying contact time and the initial dye concentration. The physicochemical properties of the adsorbent were determined using X-ray diffraction (XRD), Fourier transform infrared spectroscopy (FTIR), scanning electron microscopy (SEM), energy dispersive X-ray spectroscopy (EDX), N_2 adsorption-desorption isotherm, diffuse reflectance UV-vis spectroscopy (UV-vis DRS) and X-ray absorption near edge structure (XANES). Langmuir, Freundlich and Temkin isotherms were applied to study the adsorption phenomena.

Materials and Methods

Materials

All chemicals used in the current study were of analytical grade and thus employed as received. Distilled water was used throughout the experiments. A fresh solution of MV of the highest quality available was provided by Sigma-Aldrich and was used without further purification. Chemicals and reagents used in this work included $Ce(NO_3)_3 \cdot 6H_2O$, $Al_2(SO_4)_3 \cdot 18H_2O$, $AgNO_3$, polyethylene glycol (PEG, Mw = 20,000), NH_4OH, n-C_4H_9OH, KH_2PO_4, KOH, $NaH_2PO_4 \square H_2O$, Na_2HPO_4, H_3PO_4, H_3BO_3 and NaOH purchased from Merck, Germany. A fresh stock solution of MV dye was prepared by dissolving weighed amounts of MV with distilled water. A borate buffer solution of pH9.0 was prepared (European Pharmacopoeia 5.0, 2012).

Preparation of Adsorbent

$Ce_{0.3}Al_{0.7}$ and $Ce_{0.3}Al_{0.7}Ag_x$ (x = 0.1, 0.3 & 0.5) were prepared using a co-precipitation method based on Phatai and Futalan (2016). In this method, 1.6283 g of $Ce(NO_3)_3 \cdot 6H_2O$, 2.9157 g of $Al_2(SO_4)_3 \cdot 18H_2O$ and various amounts of $AgNO_3$ to obtain the desired molar ratios were dissolved in water and mixed under constant stirring. 1.0 g of PEG was added and the NH_4OH solution was then dropped into the mixture to attain the required pH of 9.0±0.1. The solution was continuously stirred for 2 h. Each solution was frozen at about 0°C for 24 h and the resulting gel was filtered. Next, the precipitates were washed repeatedly with distilled water and nbutanol to remove the unreacted species. The samples were initially dried in an oven at 120°C for 2 h and the resulting powder was calcined in air at 600°C for 4 h. The dried powder was then stored in a desiccator. $Ce_{0.3}Al_{0.7}$ is referred to as CeAl and the $Ce_{0.3}Al_{0.7}Ag_x$ (x = 0.1, 0.3 & 0.5) compounds are referred to as CeAlAg01, CeAlAg03 and CeAlAg05, respectively.

Equipment

The crystal structure of the samples was confirmed using XRD (Bruker D8 ADVANCE Series 2) with Cu Kα radiation source (λ = 0.15406 nm) scanning from 2θ = 20-80° with an accelerating voltage of 40 kV and current of 40 mA. FTIR spectra of fresh and spent mixed oxides were obtained using a FTIR (Spectrum Two-Perkin Elmer) over the spectral range of 4000-500 cm^{-1} using the attenuated total reflectance mode. Micrographs of the materials were obtained using SEM (Hitachi S-3000N) with an accelerating voltage of 5 kV. In order to increase the conductivity of the samples, they were gold coated using a K500X Sputter Coater at a pressure of 9×10^{-2} mbar and current of 20 mA for 5 min prior to taking SEM. Elemental contents were determined using EDX (Hitachi S-3000N). N_2 adsorption-desorption isotherms were obtained on a Quantachrome (Model Autosorb 1 MP). Before the measurement, each sample was degassed at 200°C under vacuum for 24 h. The analyses were performed at liquid nitrogen temperature. Specific surface area and average pore diameter were calculated using the Brunauer, Emmett and Teller method from the adsorption data. The electronic structure of the bulk mixed oxides was obtained using UV-vis DRS (Lamda 35, Perkin Elmer) equipped with a reflectance attachment which used a $BaSO_4$ coated integration sphere. A UV-vis spectrophotometer (Hitachi U-2900) was employed to monitor adsorption of MV dye. The form of sulfur in each adsorbent was analyzed by S K-edge XANES at room temperature in fluorescent mode at the beamline 5.2 of the Synchrotron Light Research Institute, Thailand. Each sample was pressed into a frame covered by polyimide tape and mounted onto a sample holder. Normalization of the XANES spectra was carried out using ATHENA program and compared to a reference material, $Fe_2(SO_4)_3$.

BATCH ADSORPTION STUDIES

Typical experiments for the adsorption of MV dye on the adsorbents were done using batch techniques varying the studied parameters, i.e. contact time (15-120 min) and initial dye concentration (5-50 mg/L). The pH of MV dye solution was held constant at pH 9.0±0.1 by the buffered solution. Briefly, exactly 0.10 g of mixed oxide sample was added to a 250 mL Erlenmeyer flask followed by exactly 25 mL of the desired dye concentration. The solution was agitated at a constant speed of 150 rpm. After agitation for the desired time, the mixture was filtered using Whatman-42 filter paper. The clear filtrates were diluted and then analyzed to determine the remaining concentration of MV dye using UV-vis spectrophotometry at λ_{max} = 584 nm. The adsorption capacity was calculated as follows:

Adsorption capacity = [((C$_i$-C$_t$) × V)/W],

where C$_i$ and C$_t$ are the initial and final concentrations after a desired equilibrium time (mg/L), respectively; V is a volume of solution (mL); and W is an amount of adsorbent (g)

The isotherm experiments were performed as above, but agitation was continued for 120 min to attain equilibrium. The MV dye solution (pH 9.0±0.1) of concentrations ranging from 5-50 mg/L was used for the equilibrium test. The final MV dye concentration (C$_e$, mg/L) was determined in the equilibrated solution and equilibrium capacity (q$_e$, mg/g) was calculated using the above equation substituting C$_e$ in place of C$_t$.

RESULTS AND DISCUSSION

CHARACTERIZATIONS OF THE ADSORBENT

The XRD patterns of the mixed oxides are shown in Figure 1. It can be observed that the samples displayed the typical single phase cubic fluorite structure of CeO$_2$ with peaks at 2θ of 28.7, 33.2, 47.4, 56.0, 69.0 and 76.0° corresponding to (1 1 1), (2 0 0), (2 2 0), (3 1 1), (4 0 0) and (3 3 1) lattice planes, respectively (JCPDS Card No. 34-0394). Their space group is Fm-3m. The diffraction patterns of Ag$^+$, which normally appear at 38.1, 44.3, 64.5 and 77.3° (Aykut et al. 2013) were not observed. This implies that Al^{3+} and Ag$^+$ ions were incorporated into the crystal structure of CeO$_2$ forming a solid solution. The smaller ionic radii of Al^{3+} (0.054 nm) and Ag$^+$ (0.115 nm) compared to those of Ce^{4+} (0.097 nm) and Ce^{3+} (0.114 nm) made this possible. A similar result was reported by Xiaodong et al. (2012).

FTIR spectra of the fresh (a-d) and spent (e-h) mixed oxides are displayed in Figure 2. In Figure 2(a)-2(d), the broad band at 3053-3739 cm^{-1} was due to the stretching mode of OH$^-$ ions. The band located at 1731 cm^{-1} represents the water bending vibration mode of the physically adsorbed water (O-H) molecules. The strong band at 1167 cm^{-1} suggests Al-O and S-O stretching modes
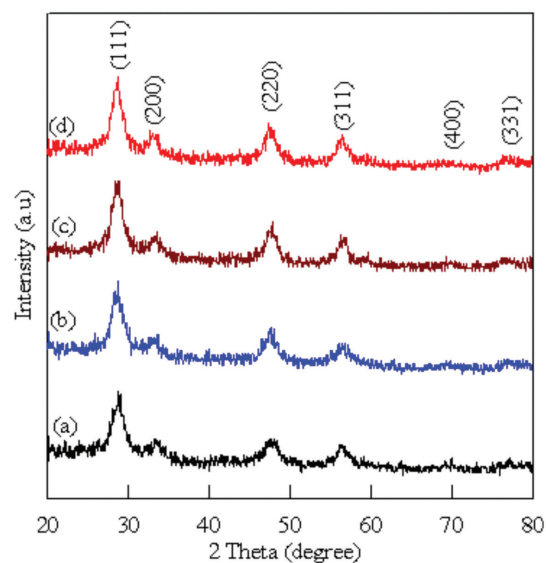

FIGURE 1. XRD patterns of mixed oxides; (a) CeAl (b) CeAlAg01 (c) CeAlAg03 and (d) CeAlAg05

(Dhonge et al. 2011; Xiaodong et al. 2012). Moreover, the weak absorption bands between 500 and 1000 cm^{-1} were attributable to the network vibrations of metal-oxygen-metal in the mixed oxide (Biswas et al. 2009) where their band intensities did not change with increasing silver content. In the spent samples (Figure 2(e)-2(h)), the intensity of all peaks decreased and the FTIR spectra of the samples showed new small peaks at ~1300-1500 cm^{-1}, which were attributable to the bending vibrations of the methyl (-CH$_2$) and methylene groups (-CH$_3$) of methyl violet dye (Akgűl & Karabakan 2011). This indicates dye insertion into the crystal structure of the mixed oxide.
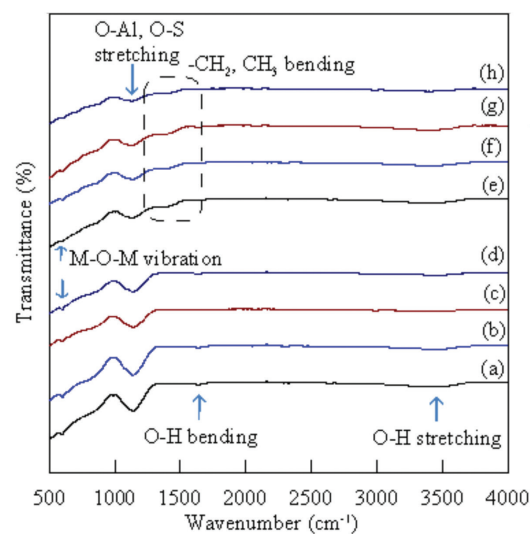

FIGURE 2. FTIR spectra of fresh mixed oxides: (a) CeAl (b) CeAlAg0 (c) CeAlAg03 (d) CeAlAg05 and spent mixed oxides: (e) CeAl (f) CeAlAg01 (g) CeAlAg03 and (h) CeAlAg05

Figure 3 shows the SEM images of CeAl and CeAlAg$_x$ samples calcined at 600°C for 4 h at ×5000 and 15000 magnifications. It was clearly observed that the small particles had a loose form, rough and porous morphology, which facilitated the adsorption of MV dye molecules into pores.

Table 1 shows the weight percentages of Ce, Al, Ag, O and S in mixed oxides derived from the large area EDX analysis. The mixed oxides consisted mainly of cerium and aluminum, while there was a little silver detected, although this increased with increasing Ag content. This supports the XRD results, where silver was not evident in
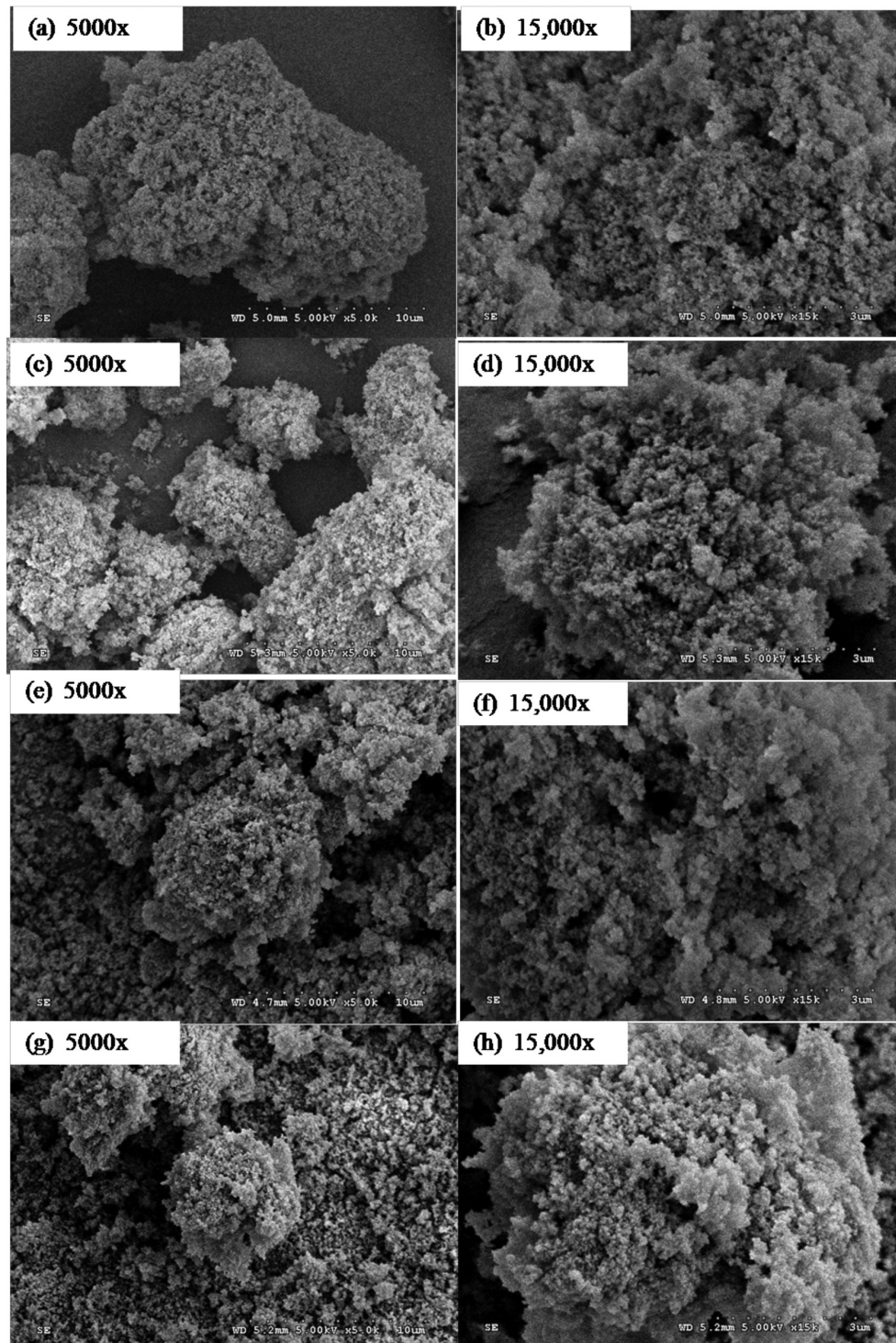

FIGURE 3. SEM images of mixed oxides at ×5,000 and 15,000 magnifications; (a, b) CeAl (c, d) CeAlAg01 (e, f) CeAlAg03 and (g, h) CeAlAg05

TABLE 1. Weight percentages of Ce, Al, Ag, O and S in mixed oxides obtained from EDX and specific surface area and average pore diameter of mixed oxides derived from N_2 adsorption-desorption isotherms

Adsorbents	% weight					Specific surface area (m^2/g)	Average pore diameter (nm)
	Ce L	Al K	Ag K	O K	S K		
CeAl	4.49	14.77	0.00	75.54	5.20	96.0	18.5
CeAlAg01	4.21	14.75	0.04	76.07	4.93	96.8	17.8
CeAlAg03	4.45	14.63	0.08	76.42	4.42	82.3	21.1
CeAlAg05	4.01	14.45	0.13	76.91	4.50	92.2	19.3

the measurements. However, the actual molar contents of each metal in CeAl and CeAlAg$_x$ oxides were lower than those of the expected nominal values due to metal loss during removal of the template (Zabilskiy et al. 2014).

The sulfur K-edge XANES spectra of the sulfur standard, CeAl and CeAlAg$_x$ mixed oxides are shown in Figure 4. The white line energy of the $Fe_2(SO_4)_3$ reference is at 2483.6 eV, which is close to those reported in literatures (Gambardella et al. 2016; Jugo et al. 2010). The sulfur K-edge XANES spectra of all adsorbents were similar to that of the $Fe_2(SO_4)_3$, indicating that the sulfur species form as a sulfate group.
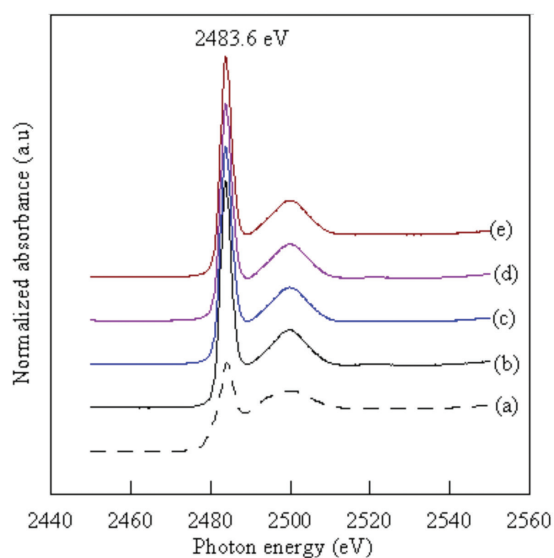
over a range of high P/P$_0$ and monolayer-multilayer adsorption features at the initial part of the isotherm. The isotherm is in agreement with the average pore diameters determined which varies in the region of 17-21 nm. The specific surface areas of CeAl and CeAlAg$_x$ vary in the region of 82-97 m^2/g. The introduction of silver ions with 0.1-0.5 molar ratio into CeAl would result in a little decrease in the specific surface area. These observed textural properties are expected to act as adsorption sites to enhance the adsorption capacity of the adsorbent for MV dyes from aqueous solution.
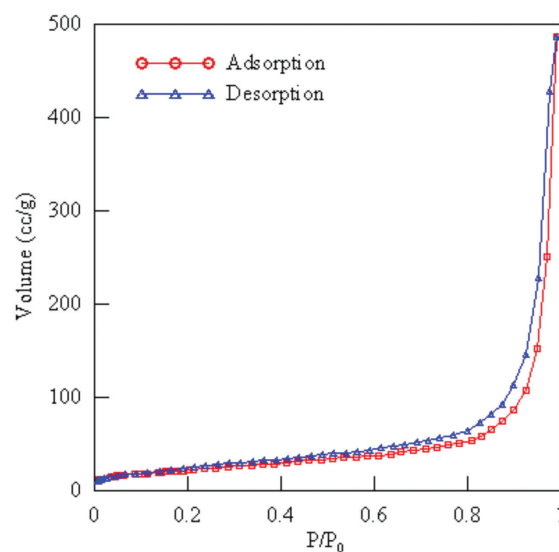

FIGURE 4. Sulfur K-edge spectra of the reference material and mixed oxides (a) $Fe_2(SO_4)_3$ (b) CeAl (c) CeAlAg01 (d) CeAlAg03 and (e) CeAlAg05

FIGURE 5. N_2 adsorption-desorption profiles of CeAl mixed oxide

The N_2 adsorption-desorption isotherm of CeAl displayed in Figure 5 is overlapped with those of CeAlAg$_x$ and their textural properties are listed in Table 1. According to IUPAC classification, all samples have type H3 hysteresis loops and correspond to a typical type IV isotherm (Wang et al. 2015; Xie et al. 2015). A rapid increase of adsorption of nitrogen can be observed when P/P$_0$ is above 0.7, implying the presence of mesopores. This physisorption isotherm is associated with the capillary condensation taking place in mesopores, a limiting uptake

The spectra of UV-vis DRS shown in Figure 6 shows the absorption of UV-visible light in the range of 200-800 nm, which is very sensitive to the coordination number of the transition metal sites. A strong absorption band around 260-330 nm was observed, indicating the charge transfer transition of O^{2-} to Ce^{3+} and Ce^{4+} (Rao & Mishra 2005). This suggests that Ce^{3+} and Ce^{4+} ions coexist within the mixed oxide lattices.

In the inset Figure 6, the maximum absorbance peak of the samples shifted to a lower wavelength as the silver content increased. It is normally called a blue shift in the absorption edge. This blue shift was clearly seen in the
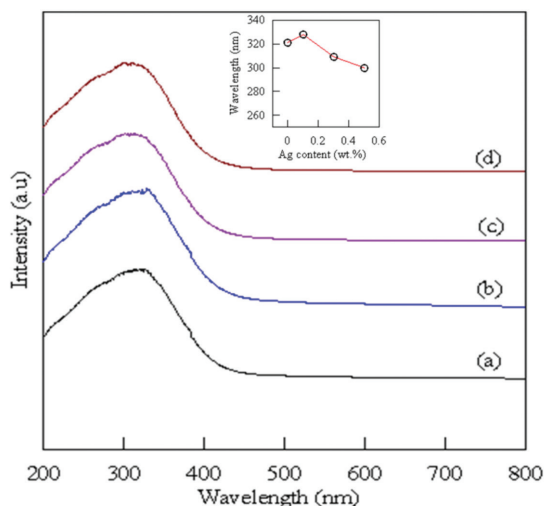
FIGURE 6. UV-vis DRS spectra of mixed oxides (a) CeAl
(b) CeAlAg01 (c) CeAlAg03 and (d) CeAlAg05

UV region and indicated that the crystalline size of CeO_2 was below 10 nm (Rao & Sahu 2011).

EFFECT OF CONTACT TIME

The effect of equilibrium contact time is shown in Figure 7 where a rapid removal of dye and the establishment of equilibrium in a short time address the efficiency of the adsorbent for its use in wastewater treatment. The adsorption rate was very high during the first 15 min because a large number of vacant active sites on the surface were available for adsorption. After this, residual vacant sites were more difficult to occupy due to repulsive forces between MV molecules adsorbed on the oxide surface and the solution phase. The equilibrium was reached at 120 min. This time was utilized throughout the entire study. Moreover, it was observed that CeAlAg05 gave lower adsorption capacity than CeAlAg03. This reversal of the rising trend with increasing Ag content could be attributed
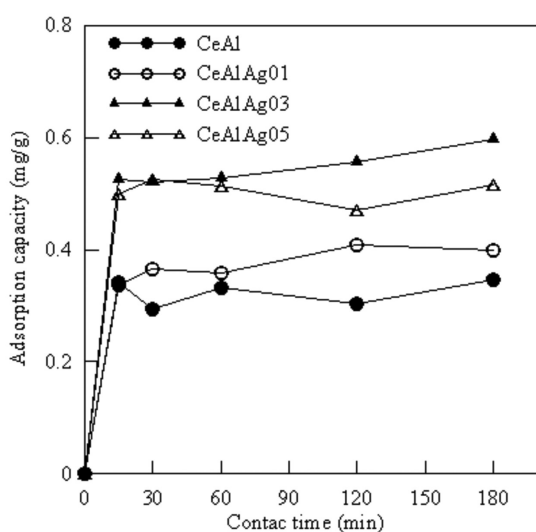

FIGURE 7. The effect of contact time on adsorption capacity by CeAl and CeAlAg$_x$ mixed oxides

to silver overdose having led to the agglomeration of silver oxide, resulting in fewer adsorption sites being available for MV dye adsorption.

EFFECT OF INITIAL CONCENTRATION

Figure 8 shows the dependence of adsorption capacities of CeAl and CeAlAg$_x$ for MV dye on their concentrations. It can be seen that the adsorption capacities were highly dependent on the initial MV concentration. When the initial MV concentration was increased, the adsorption capacity of all samples increased. It can be concluded that the greater initial dye concentration provided an important driving force for diffusion to overcome mass transfer resistances of the MV dye between the bulk solution and solid phases
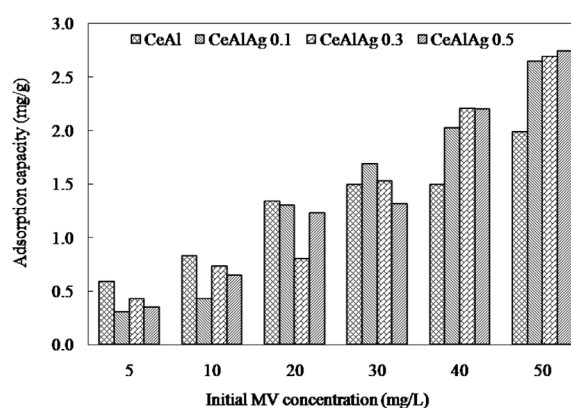

FIGURE 8. The effect of initial dye concentration on adsorption capacity by CeAl and CeAlAg$_x$ mixed oxides

(Sarici-Ozdemir 2012). A similar result was reported for the adsorption of Congo red on Ca-bentonite in work done by Lian et al. (2009) and on MFe_2O_4 (M = Mn, Fe, Co, Ni) by Wang et al. (2012).

ADSORPTION ISOTHERM MODELING

The Langmuir, Freundlich and Temkin isotherms are defined in the literature (Alshabanat et al. 2013; Phatai & Futalan 2016; Wang et al. 2012) and they were used to estimate the isothermal parameters for MV adsorption onto CeAl and CeAlAg$_x$ oxides.

The homogeneous Langmuir adsorption isotherm is represented by the following:

$$\frac{C_e}{q_e} = \frac{1}{q_m K_L} + \frac{C_e}{q_m}, \tag{1}$$

where C_e is the equilibrium concentration of dye (mg/L); q_e is the amount of dye adsorbed per unit mass of adsorbent (mg/g); q_m is the maximum monolayer capacity of dye on the adsorbent material (mg/g); and K_L is the adsorption equilibrium constant (L/mg).

The heterogeneous Freundlich adsorption isotherm is represented by the following:

$$\ln q_e = \ln K_F + \frac{1}{n}\ln C_e, \tag{2}$$

where K_F (mg/g) and n are the Frendlich constants associated with adsorption capacity and adsorption intensity of the dye onto the adsorbent, respectively.

The Temkin isotherm can be expressed by the following:

$$q_e = B\ln A + B\ln C_e, \tag{3}$$

where A is the equilibrium constant corresponding to the maximum binding energy (L/g); and B is the Temkin constant related to the heat of adsorption (kJ/mol).

Typical parameter values are given in Table 2. Based on the correlation coefficients (R^2), it was found that the Langmuir isotherm was the most suitable for modelling MV adsorption on CeAl ($R^2 = 0.9951$). This implies that the MV adsorption onto CeAl proceeds by monolayer adsorption. This result was supported by previous work (Phatai & Futalan 2016). In contrast, the adsorption data for all CeAlAg$_x$ oxides was best fitted by the Frendlich isotherm, indicating multilayer adsorption of MV molecules onto the adsorbents. This signifies that the MV dye was adsorbed onto different binding sites such as M-OH and M-O-M (M = Ce, Al and Ag) as reported by Phatai and Futalan (2016).

Based on these experimental results, the maximum q_m value in the current study using CeAl (2.35 mg/g) was lower than that of CeAl (25 mg/g) from the previous work (Phatai & Futalan 2016) under the same experimental conditions. This result can be attributed to the type of precursor and its effect on adsorption capacity. CeAl oxide from the previous work (Phatai & Futalan 2016) was prepared using nitrate precursors of Ce and Al, while the adsorbents used in this work was obtained from a sulfate compound of Al and nitrate compounds of Ce and Ag. Sulfur present in the mixed oxide (4-5 wt. %) as detected in the EDX and XANES results was not eliminated by calcination at 600°C. Thus, sulfur formed sulfur oxide in the mixed oxide lattice, decreased surface area and may block the active sites for adsorption of MV molecules. This was referred to as sulfur poisoning, which was widely studied in catalysis reactions. Xiaodong et al. (2012) reported that formation of sulfate on the surface of a MnO$_x$-CeO$_2$-Al$_2$O$_3$ catalyst resulted in loss of surface active sites, thereby deactivating NO$_x$ oxidation. The effect of sulfur content in mixed oxides for the adsorption of MV dye will be further investigated.

POSSIBLE ADSORPTION MECHANISM

Based on the characteristics of the mixed oxide and MV dye, the mechanisms of MV adsorption by the oxides are somewhat complex. MV dye is a cationic dye, while the CeAl and CeAlAg ternary mixed oxides have amphoteric surfaces, depending upon the pH of their solution. At pH9.0, the mixed oxides formed negative charges. Thus,

TABLE 2. Isotherm model parameters obtained for MV adsorption onto CeAl and CeAlAg$_x$

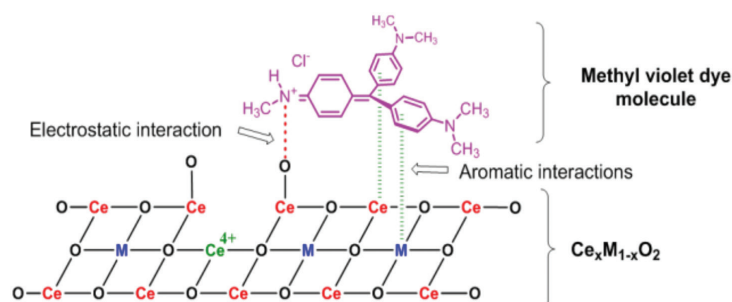| Isotherms	Parameters	Adsorbents			
		CeAl	CeAlAg0.1	CeAlAg0.3	CeAlAg0.5
Langmuir	q_m (mg/g)	2.3458	5.1787	6.5147	7.2886
	K_L (L/mg)	0.3126	0.0843	0.0340	0.0300
	R^2	0.9951	0.4556	0.3276	0.3870
Freundlich	K_F (mg/g)	0.6460	1.8481	0.2892	0.2431
	n (g/L)	2.2655	0.6357	1.3548	1.2006
	R^2	0.9431	0.7839	0.9301	0.9396
Temkin	B (kJ/mol)	0.5059	0.9295	0.8881	0.9559
	A (L/g)	3.1733	1.4500	0.7474	0.6871
	R^2	0.9790	0.6032	0.8408	0.8874

FIGURE 9. Possible adsorption mechanism of MV adsorption onto CeAl and CeAlAg$_x$ mixed oxide

the electrostatic interaction between O^{2-} sites of mixed oxides and N^+HR_2 dye (Figure 9) would be the major adsorption mechanism. In this case, MV dye from the bulk solution migrated to the oxide surface and finally into the pores of the adsorbent. This phenomenon was previously reported (Tan et al. 2015; Zeng et al. 2014). Moreover, the π-π or aromatic interactions of benzene rings and metal ions and hydrogen bonding between the adsorbent and adsorbate could have taken place. Even if the result from FTIR did not demonstrate O^{2-}-N^+HR_2 dye interaction, it confirmed the insertion of the MV dye into the pores of the mixed oxides.

CONCLUSION

In the current study, samples of CeAl and CeAlAg$_x$ oxides with different molar ratios of silver ions were successfully prepared using a co-precipitation technique. The physicochemical properties of the adsorbents were determined using several techniques. The results showed that all metal ions were homogeneously incorporated into a cubic fluorite structure of CeO_2 with a rough texture and porous morphology. FTIR confirmed the functional groups in fresh and spent adsorbents and the insertion of MV dye molecules into the mixed oxides. The equilibrium adsorption time was 120 min and increasing the initial MV concentration increased adsorption capacity. The Langmuir isotherm model gave the best fit for the adsorption of MV dye onto $Ce_{0.3}Al_{0.7}$, yielding a maximum adsorption capacity of 2.35 mg/g. In contrast, the Freundlich model best depicted MV dye adsorption onto CeAlAg$_x$. The possible adsorption mechanisms of MV dyes onto the CeAl and CeAlAg$_x$ may have been due to electrostatic interaction, π-π interactions between benzene rings of MV dye and metal ions, and hydrogen bonding.

REFERENCES

Akgűl, M. & Karabakan, A. 2011. Promote dye adsorption performance over desilicated natural zeolite. *Microporous Mesoporous Materials* 145: 157-164.

Alshabanat, M., Alsenani, G. & Almufarij, R. 2013. Removal of crystal violet dye from aqueous solution onto date palm fiber by adsorption technique. *Journal of Chemistry* 2013: Article ID 210239.

Aykut, Y., Pourdeyhimi, B. & Khan, S.A., 2013. Synthesis and characterization of silver/lithium cobalt oxide ($Ag/LiCoO_2$) nanofibers via sol-gel electrospinning. *J. Phys. Chem. Solid* 74: 1538-1545.

Biswas, K., Gupta, K. & Ghosh, U.C. 2009. Adsorption of fluoride by hydrous iron (III)-tin (IV) bimetal mixed oxide from the aqueous solutions. *Chemical Engineering Journal* 149: 196-206.

Debnath, S., Kitinya, J. & Onyango, M.S. 2014. Removal of Congo red from aqueous solution by two variants of calcium and iron based mixed oxide nano-particle agglomerates. *Journal of Industrial and Engineering Chemistry* 20: 2119-2129.

Deniz, F. 2013. Adsorption properties of low-cost biomaterial derived from *Prunus amygdalus* L. for dye removal from water. *The Scienctific World Journal* 2013: Article ID 961671.

Dhonge, B.P., Mathews, T., Sundari, S.T., Thinaharan, C., Kamruddin, M., Dash, S. & Tyagi A.K. 2011. Spray pyrolytic deposition of transparent aluminum oxide (Al_2O_3) films. *Applied Surface Science* 258: 1091-1096.

Gambardella, A.A., Schmidt Patterson, C.M., Webb, S.M. & Walton, M.S. 2016. Sulfur K-edge XANES of lazurite: Toward determining the provenance of lapis lazuli. *Microchemical Journal* 125: 299-307.

Guimarães, J.R., Maniero, M.G. & de Araújo, R.N. 2012. A comparative study on the degradation of RB-19 dye in an aqueous medium by advanced oxidation processes. *Journal of Environmental Management* 110: 33-39.

Jiao, F., Yu, J., Song, H., Jiang, X., Yang, H., Shi, S., Chen, X. & Yang, W. 2014. Excellent adsorption of acid flavine 2G by MgAl-mixed metal oxides with magnetic iron oxide. *Applied Clay Science* 101: 30-37.

Jugo, P.J., Wilke, M. & Botcharnikov, R.E. 2010. Sulfur K-edge XANES analysis of natural and synthetic basaltic glasses: Implications for S speciation and S content as function of oxygen fugacity. *Geochimica et Cosmochimica Acta* 74: 5926-5938.

Kongkachuichay, P., Shitangkoon, A. & Hirunkitmonkon, S. 2010. Thermodynamics study of natural indigo adsorption on silk yarn. *Chiangmai Journal of Science* 37: 363-367.

Lian, L., Guo, L. & Guo, C. 2009. Adsorption of Congo red from aqueous solutions onto Ca-bentonite. *Journal of Hazardous Materials* 161: 126-131.

Mittal, A., Gajbe, V. & Mittal, J. 2008. Removal and recovery of hazardous triphenylmethane dye, methyl violet through adsorption over granulated waste materials. *Journal of Hazardous Materials* 150: 364-375.

Monash, P. & Pugazhenthi, G. 2009. Adsorption of crystal violet dye from aqueous solution using mesoporous materials synthesized at room temperature. *Adsorption* 15: 390-405.

Phatai, P. & Futalan, C.M. 2016. Removal of methyl violet dye by adsorption onto mesoporous mixed oxides of cerium and aluminum. *Desalination and Water Treatment* 57: 8884-8893.

Phatai, P., Utara, S. & Hatthapanit, N. 2014. Removal of methyl violet by adsorption onto activated carbon derived from coffee residues. *Advanced Materials Research* 864-867: 710-714.

Rao, G.R. & Sahu, H.R. 2011. XRD and UV-Vis diffuse reflectance analysis of CeO_2-ZrO_2 solid solutions synthesized by combustion method. *Proceedings of the Indian Academy of Sciences* 113: 651-658.

Rao, G.R. & Mishra, B.G., 2005. A comparative UV-vis-diffuse reflectance study on the location and interaction of cerium ions in Al- and Zr-pillared montmorillonite clays. *Materials Chemistry and Physics* 89(1): 110-115.

Sarici-Ozdemir, C. 2012. Adsorption and desorption kinetics behavior of methylene blue onto activated carbon.

Physicochemical Problems of Mineral Processing 48: 441-454.

Subramaniam, R. & Ponnusamy, S.K. 2015. Novel adsorbent from agricultural waste (cashew NUT shell) for methylene blue dye removal: Optimization by response surface methodology. *Water Resources and Industry* 11: 64-70.

Tan, K.B., Vakili, M., Horri, B.A., Poh, P.E., Abdullah, A.Z. & Salamatinia, B. 2015. Adsorption of dyes by nanomaterials: Recent developments and adsorption mechanisms. *Separation and Purification Technology* 150: 229-242.

Tapalad, T., Neramitagapong, A., Neramitgapong, S. & Boonmee, M. 2008. Degradation of congo red dye by ozonation. *Chiang Mai Journal of Science* 35: 63-68.

Wang, D., Zhang, X., Liu, C., Cheng, T., Wei, W. & Sun, Y. 2015. Transition metal-modifies mesoporous Mg-Al mixed oxides: Stable base catalysts for the synthesis of diethyl carbonate from ethyl carbamate and ethanol. *Applied Catalysis A: General* 505: 478-486.

Wang, L., Li, J., Wang, Y., Zhao, L. & Jiang, Q. 2012. Adsorption capacity for Congo red on nanocrystalline MFe_2O_4 (M = Mn, Fe, Co, Ni) spinel ferrites. *Chemical Engineering Journal* 181-182: 72-79.

Wawrzkiewicz, M., Wiśniewska, M., Gun'ko, V.M. & Zarko, V.I. 2015. Adsorptive removal of acid, reactive and direct dyes from aqueous solutions and wastewater using mixed silica-alumina oxide. *Powder Technology* 278: 306-315.

Xiaodong, W., Hyeing-Ryeol, L., Shuang, L. & Duan, W. 2012. Sulfur poisoning and regeneration of MnO_x-CeO_2-Al_2O_3 catalyst for soot oxidation. *Journal of Rare Earths* 30: 659-664.

Xie, Y., Wang, J., Wang, M. & Ge, X. 2015. Fabrication of fibrous amidoxime-fuctionalized mesoporous silica microsphere and its selectively adsorption property for Pb2+ in aqueous solution. *Journal of Hazardous materials* 297: 66-73.

Zabilskiy, M., Erjavec, B., Djinovic, P. & Pintar, A. 2014. Ordered mesoporous CuO-CeO_2 mixed oxides as an effective catalyst for N_2O decomposition. *Chemical Engineering Journal* 254: 153-162.

Zaini, M.A.A., Meng, T.W., Johari Kamaruddin, M., Septapar, S.H.M. & Azizi Che Yunus, M. 2014. Microwave-induced zinc chloride active palm kernel shell for dye removal. *Sains Malaysiana* 43(9): 1421-1428.

Zeng, S., Duan, S., Tang, R., Li, L., Liu, C. & Sun, D. 2014. Magnetically separable $Ni_{0.6}Fe_{2.4}O_4$ nanoparticles as an effective adsorbent for dye removal: Synthesis and study on the kinetic and thermodynamic behaviors for dye adsorption. *Chemical Engineering Journal* 258: 218-228.

Phatai, P.* & Srisomang, R.
Department of Chemistry, Faculty of Science
Udon Thani Rajabhat University
Udon Thani, 41000
Thailand

Phatai, P.* & Srisomang, R.
Polymer and Material Research Groups
Faculty of Science, Udon Thani Rajabhat University
Udon Thani, 41000
Thailand

*Corresponding author; email: piawtee99@hotmail.com